1
Electronic Structure and Magnetic Properties of Lanthanide Molecular Complexes

Lorenzo Sorace and Dante Gatteschi

1.1
Introduction

The first studies on the magnetic and electronic properties of compounds containing lanthanide ions date back to the beginning of the twentieth century [1]. However, detailed investigation on these systems only began in the $50s^2$ and helped set up an appropriate theoretical framework for the analysis of their properties [2–5]. Most of the studies reported in the early literature, which involved optical spectroscopy, magnetism, or electron paramagnetic resonance (EPR), were however concerned with inorganic systems in which the lanthanide occupied high symmetry sites, and paramagnetic ions were often doped in diamagnetic host lattices [6, 7].

On the other hand, the number of molecular complexes (which usually show a low point symmetry at the lanthanide site) whose magnetic properties had been well characterized remained quite small even in 1993, when Kahn [8] wrote his landmark book entitled *Molecular Magnetism*. The field of lanthanide molecular magnetism has indeed really boomed only in the last 15 years, when the availability of powerful theoretical and experimental techniques allowed deep insight into these systems. As a result, some more specific applications of the theory that was developed for inorganic systems to the molecular magnets case were needed. The purpose of this chapter is to describe the fundamental factors affecting the electronic structure of lanthanide complexes, with some specific focus on the symmetry, and the way this is related to their static magnetic properties (dynamic magnetic properties being the focus of a subsequent chapter).

Lanthanide atoms in the electronic ground state are characterized by the progressive filling of 4f shells, with the general configuration $[Xe]4f^n6s^2$ (with the exception of La, Ce, Gd, Lu, for which the ground configuration is $[Xe]4f^n5d^16s^2$). For this reason, the most stable lanthanide ions are the tripositive ones, obtained by loss of the 5d and 6s electrons (notable exceptions are Eu^{2+}, Ce^{4+} and Tb^{4+},

Lanthanides and Actinides in Molecular Magnetism, First Edition.
Edited by Richard A. Layfield and Muralee Murugesu.

which have stable electronic configurations). In the following, we discuss the paramagnetic properties of rare earth compounds arising from the unpaired 4f electrons: since these are effectively shielded by the completely filled 5s and 5p orbitals, their behaviour is much less affected by the coordination environment of the ion compared to the 3d transition metal series. Consequently, optical spectra consist of very sharp, weak lines due to formally forbidden 4f–4f transitions, while the magnetic properties can, to a first approximation, be expressed as those of a free Ln^{3+} ion. This means that rare earth ions present an essentially unquenched orbital momentum, since the core-like character of 4f orbitals (compared, e.g. to 3d ones) prevents the crystal field (CF) from quenching the orbital momentum.[1)] For this reason, in the early days of magnetochemistry, lanthanides were studied as a model of free ions, much more accessible than the paramagnetic gases [9].

The first attempts to rationalize the magnetic properties of rare earth compounds date back to Hund [10], who analysed the magnetic moment observed at room temperature in the framework of the 'old' quantum theory, finding a remarkable agreement with predictions, except for Eu^{3+} and Sm^{3+} compounds. The inclusion by Laporte [11] of the contribution of excited multiplets for these ions did not provide the correct estimate of the magnetic properties at room temperature, and it was not until Van Vleck [12] introduced second-order effects that agreement could be obtained also for these two ions.

The effect of the coordinating ligands over the magnetic properties of lanthanides becomes important in lowering the temperature, as the ground multiplets are split by an amount comparable to thermal energy: as a consequence, depopulation of the sublevels occurs, and deviation from the Curie law is observed. This, in turn, complicates the interpretation of magnetic properties of systems in which the lanthanide(III) ion interacts with another paramagnetic species. Indeed, effects due to the magnetic exchange are very small – because the unpaired electrons are in the well-shielded f orbitals – and may be hidden by ligand field effects at low temperature. It is, then, of paramount importance to appropriately determine the split components of the lowest lying multiplet and to understand the factors on which this depends.

In the following sections, we start by discussing in some detail the electronic structure of the free ion, following the classic treatment of Wybourne [3], and we successively analyse the effect of the ligand field. The relation between the Stevens' formalism [2], to which the molecular magnetism community is more used, and Wybourne's notation is presented. Indeed, the latter takes more easily into account the effect of the excited multiplets, and its use might facilitate interchange and data comparison with results from luminescence and absorption spectroscopy. The resulting magnetic properties and EPR spectra are discussed,

1) Exceptions to this behaviour are Eu^{2+} and Gd^{3+}, which – as a consequence of their $4f^7$ electronic configuration – present an orbitally non-degenerate ground state.

with some examples from more recent literature. Finally, we briefly discuss the way exchange coupling effects are treated in molecular systems containing anisotropic lanthanides.

1.2 Free Ion Electronic Structure

We start our description of the electronic structure of complexes of lanthanides by the analysis of the free ion energy structure. The relevant Hamiltonian is written as

$$\hat{\boldsymbol{H}} = \sum_{k=1}^{n} \left\{ \frac{1}{2m}\boldsymbol{p}_{\boldsymbol{k}}^2 - \frac{Ze^2}{r_k} \right\} + \sum_{k=1}^{n} \zeta(r_k)\boldsymbol{l}_{\boldsymbol{k}} \cdot \boldsymbol{s}_{\boldsymbol{k}} + \sum_{k<\lambda}^{n} \frac{e^2}{r_{k\lambda}} \tag{1.1}$$

In Equation 1.1, the first term is the sum of hydrogen-like terms for single electrons and the second one is the sum of the single-electron spin–orbit interaction, while the third term contains the interelectronic repulsion. By applying the central field approximation [13], each single electron can be considered as moving in an average, spherically symmetric field due to the nucleus and to the remaining electrons:

$$\hat{\boldsymbol{H}}_0 = \sum_{k=1}^{n} \left\{ \frac{1}{2m}\boldsymbol{p}_{\boldsymbol{k}}^2 + U\left(r_k\right) \right\} \tag{1.2}$$

This allows separation of the corresponding Schrödinger equation in n independent equations, one for each electron, so that the solution of Equation 1.2 will be a product of functions of the type:

$$\Psi(k) = r^{-1}R_{nl}\left(r\right)Y_l^m(\theta, \varphi) \tag{1.3}$$

In Equation 1.3, the radial function $R_{nl}\left(r\right)$ is defined by the quantum numbers n and l and the spherical harmonics Y_l^m depend on the quantum numbers l and m_l. When the spin of the electron is taken into account, the normalized antisymmetric function is written as a Slater determinant. The corresponding eigenvalues depend only on n and l of each single electron, which determine the electronic configuration of the system.

The difference $\hat{\boldsymbol{H}}_1$ between the Hamiltonians (1.1) and (1.2):

$$\hat{\boldsymbol{H}}_1 = \sum_{k=1}^{n} \left\{ -\frac{Ze^2}{r_k} - U\left(r_k\right) \right\} + \sum_{k=1}^{n} \zeta(r_k)\boldsymbol{l}_{\boldsymbol{k}} \cdot \boldsymbol{s}_{\boldsymbol{k}} + \sum_{k<\lambda}^{n} \frac{e^2}{r_{k\lambda}} \tag{1.4}$$

can now be treated as a perturbation, the first term of which only causes a global shift of the energies without affecting the relative differences. Both the second and the third terms split each configuration into separate multiplets, since their effect is different for different states of the same configuration.

Within this framework it is assumed that the energy differences between each configuration are much higher than the splitting induced through Equation 1.4, so that each configuration is treated separately. The calculation of the matrix element of $\hat{\boldsymbol{H}}_1$ is obtained after defining a set of basis states in a specified angular momenta coupling scheme: this corresponds to assigning a different relative importance to the second and third terms of Equation 1.4, that is, respectively the spin–orbit and the interelectronic repulsion interactions. If the former dominates over the latter, the j–j coupling scheme is applied, in which the spin $\boldsymbol{s_i}$ and the angular momenta $\boldsymbol{l_i}$ of each electron are first coupled to provide a global momentum $\boldsymbol{j_i}$. This is done following the rules of angular momentum addition, so that $|\boldsymbol{l_i} - \boldsymbol{s_i}| < \boldsymbol{j_i} < \boldsymbol{l_i} + \boldsymbol{s_i}$. After this, the $\boldsymbol{j_i}$ values of each electron are coupled to obtain a global $\boldsymbol{J}$.

The former scheme is usually applied to heavy atoms, while for rare-earth ions the LS coupling scheme (also known as *Russell–Saunders coupling*) is normally used. In this approach, interelectronic repulsion is considered to be dominant over spin–orbit coupling. As a consequence, the spins of all the electrons are first coupled together to obtain a global spin $\boldsymbol{S} = \sum_i \boldsymbol{s_i}$, and the same is done with angular momenta $\boldsymbol{L} = \sum_i \boldsymbol{l_i}$. The corresponding matrix elements of the interelectronic repulsion Hamiltonian are then diagonal with respect to S, L, M_S, M_L and are independent of the latter, providing a $[(2S+1)(2L+1)]$-fold degenerate set of states. This set of states is called a *term*, and is characterized by n, l, S and L quantum numbers (where the first two values are fixed to 4 and 3 for 4f electrons), and the term is indicated by a ${}^{2S+1}L$ symbol, with S, P, D, F, … etc. corresponding to $L = 0, 1, 2, 3, \ldots$ etc. However, terms characterized by the same $|S, L, M_S, M_L\rangle$ may appear more than once in a given configuration, so that this set of quantum numbers is not always sufficient to characterize the term unambiguously. For this purpose, Racah introduced the irreducible representations of the groups R_7 and G_2, indicated by W and U, respectively [14].

The interelectronic repulsion Hamiltonian also commutes with $\boldsymbol{J} = \boldsymbol{S} + \boldsymbol{L}$, so that its matrices are diagonal also with respect to J and M_J, the corresponding eigenvalues being independent of M_J. Since states of $|J, M_J\rangle$ are linear combinations of $|S, L, M_S, M_L\rangle$ states with the same S, L in the scheme $|S, L, J\rangle$ the energy is also independent of J. There then exist two sets of functions depending on the quantum numbers ($|S, L, M_S, M_L\rangle$ and $|S, L, J, M_J\rangle$) in which the interelectronic repulsion is diagonal, whose energies depend only on S and L.

The labelling of terms as $|S, L, J, M_J\rangle$ is preferable when one takes into account the effect of spin–orbit coupling, since J and M_J remain good quantum numbers even after this perturbation is accounted for. In detail, the effect of spin–orbit coupling over a many-electron atomic term is evaluated by writing the spin–orbit operator in terms of the total angular and spin momentum, $\boldsymbol{L}$ and $\boldsymbol{S}$:

$$\hat{H}_{s.-o.} = \sum_{k=1}^{n} \zeta(r_k) \boldsymbol{l_k} \cdot \boldsymbol{s_k} = \lambda \boldsymbol{L} \cdot \boldsymbol{S} \tag{1.5}$$

In Equation 1.5, λ is the spin–orbit coupling within a given Russell–Saunders multiplet, which is related to the spin–orbit coupling constant of the ion, ζ, by the relation $\lambda = \pm\zeta/2S$, the + sign applying for $n < 7$ and the − sign for $n > 7$ [15]. The effect of spin–orbit coupling is to split the terms in multiplets with same L, S and different values of J, with energies $E(^{2S+1}L_J) = (\lambda/2)[J(J+1) - L(L+1) - S(S+1)]$, so that the ground state is $J = L - S$ for $n < 7$ and $J = L + S$ for $n > 7$. The important point is that the ground state corresponds to different orientation of the spins with respect to the angular orbital momentum: antiparallel for $n < 7$ and parallel for $n > 7$. As we will see, this has paramount importance for the magnetic properties throughout the lanthanide series. The remaining $2J + 1$ (Figure 1.1) degeneracy can only be removed by a further perturbation: either by a magnetic field, or by the ligand field, the effect of which is considered in the following sections.

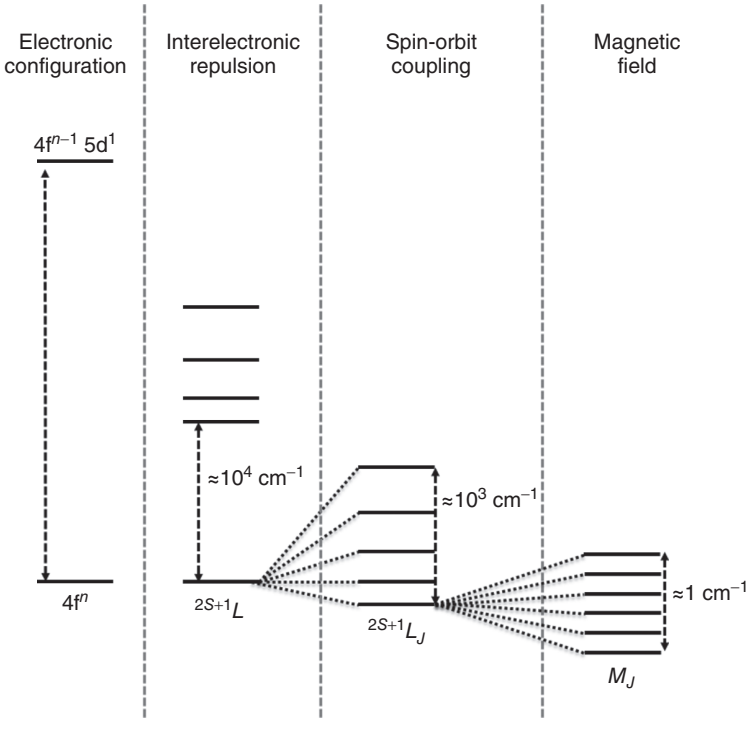

Figure 1.1 Effect of interelectronic repulsion, spin–orbit coupling and magnetic field on the energy levels arising from a given $4f^n$ configuration for a free-ion Ln^{3+}. The magnetic field effect is estimated assuming a 1 T field.

1.2.1 Free Ion Magnetism

By applying a magnetic field, the degeneracy of the $(2J + 1)$ levels in each $^{2S+1}L_J$ multiplet is removed, providing a series of levels identified by their M_J value, with $-J \leq M_J \leq +J$. The corresponding field-dependent energy can be written in terms of a Landé splitting factor, g_J, depending on J, L and S. The value of this factor as a function of J, L and S can be obtained by considering that the corresponding magnetic moment will be

$$\mu_J = \mu_B g_J \boldsymbol{J} = \mu_B (g_L \boldsymbol{L} + g_S \boldsymbol{S}) \tag{1.6}$$

One can thus write the following equality for the diagonal matrix elements of $\mu_J \cdot \boldsymbol{J}$:

$$\left\langle J, M_J \middle| \mu_J \cdot \boldsymbol{J} | J, M_J \right\rangle = \mu_B g_J \langle J, M_J | \boldsymbol{J} \cdot \boldsymbol{J} | J, M_J \rangle \tag{1.7}$$

The second term of Equation 1.7 may be rewritten, making use of Equation 1.6, as

$$\begin{aligned} \mu_B \left(g_L \boldsymbol{L} \cdot \boldsymbol{J} + g_S \boldsymbol{S} \cdot \boldsymbol{J} \right) = \mu_B \Big[& g_L \left(\boldsymbol{L}^2 + \frac{1}{2} \left(\boldsymbol{J}^2 - \boldsymbol{L}^2 - \boldsymbol{S}^2 \right) \right) \\ & + g_S \left(\boldsymbol{S}^2 + \frac{1}{2} \left(\boldsymbol{J}^2 - \boldsymbol{L}^2 - \boldsymbol{S}^2 \right) \right) \Big] \end{aligned} \tag{1.8}$$

which finally yields

$$g_J = \frac{g_L(L(L+1) + J(J+1) - S(S+1)) + g_S(S(S+1) + J(J+1) - L(L+1))}{2J(J+1)} \tag{1.9}$$

Since $g_L = 1$ and assuming for the sake of simplicity $g_S = 2$, one obtains

$$g_J = \frac{3}{2} + \frac{S(S+1) - L(L+1)}{2J(J+1)} \tag{1.10}$$

For $J = 0$ there is obviously no first-order Zeeman splitting: however, application of a magnetic field can result in second-order splitting. As such, it is necessary to evaluate the corresponding g_J factor, which is $g_0 = 2 + L(2 + S)$.

The magnetic susceptibility of the free ion will follow the Curie law:

$$\chi^M = \frac{N_A g_J^2 \mu_B^2}{3kT} J(J+1) \tag{1.11}$$

where χ^M is the molar magnetic susceptibility and N_A is the Avogadro number. This situation is indeed experimentally observed for Ln^{3+} complexes at room temperature, where the measured magnetic moment coincides with what is expected for the free-ion Curie behaviour, provided that the ground J multiplet is well isolated from the excited states (see Table 1.1). This is not the case both for Eu^{3+} – whose first excited state $^7F_1$ is lying only at ca 350 cm^{-1} above the non-magnetic $^7F_0$ ground state – and Sm^{3+}, for which the first excited state $^6H_{7/2}$ is lying about 700 cm^{-1} above the ground $^6H_{5/2}$ state [10].

Table 1.1 Relevant magnetic information for free Ln^{3+} ions.

Ion	Ground multiplet	S	L	J	g	χT value calculated	χT value experimental
Ce^{3+}	$^2F_{5/2}$	1/2	3	5/2	6/7	0.80	0.82
Pr^{3+}	$^3H_4$	1	5	4	4/5	1.60	1.54
Nd^{3+}	$^4I_{9/2}$	3/2	6	9/2	8/11	1.64	1.57
Pm^{3+}	$^5I_4$	2	6	4	3/5	0.90	Not measured
Sm^{3+}	$^6H_{5/2}$	5/2	5	5/2	2/7	0.09 (0.31)	0.27
Eu^{3+}	$^7F_0$	3	3	0	0	0 (1.5)	1.40
Gd^{3+}	$^8S_{7/2}$	7/2	0	7/2	2	7.87	8.10
Tb^{3+}	$^7F_6$	3	3	6	3/2	11.82	11.33
Dy^{3+}	$^6H_{15/2}$	5/2	5	15/2	4/3	14.17	13.91
Ho^{3+}	$^5I_8$	2	6	8	5/4	14.07	13.52
Er^{3+}	$^4I_{15/2}$	3/2	6	15/2	6/5	11.48	11.28
Tm^{3+}	$^3H_6$	1	5	6	7/6	7.15	6.51
Yb^{3+}	$^2F_{7/2}$	1/2	3	7/2	8/7	2.57	2.49

For Sm^{3+} and Eu^{3+} the χT values (given in emu kelvin per mole) obtained by including the Van Vleck contribution are reported in brackets. The experimental values refer to the $Ln_2(SO_4)_3 \cdot 8H_2O$ series, obtained as an average of the different measurements reported by Van Vleck [9].

For the latter two ions, the presence of low-lying excited states makes the inclusion of both the first-order contribution of the excited states and the second-order effects due to coupling of the ground J state with the excited states crucial in a correct estimation of the room-temperature values of χT. Indeed, second-order contribution in Van Vleck [9] expansion of the susceptibility is inversely proportional to the energy difference between the ground and the excited states:

$$\chi_{VV} = -2N \sum_{M_J=-J}^{J} \sum_{J'=-M'_J}^{-M'_J} \frac{\langle J, M_J | \mu_B (\boldsymbol{L} + g_S \boldsymbol{S}) | J', M'_J \rangle}{E_{J,M_J} - E_{J',M'_J}} = \frac{2N\mu_B^2 (g_J - 1)(g_J - 2)}{3\lambda} \quad (1.12)$$

1.3 Electronic Structure of Lanthanide Ions in a Ligand Field

When a lanthanide ion is placed in a ligand environment with symmetry lower than spherical, the energies of its partly filled 4f orbitals are split by the electrostatic field of the ligand. The result is a splitting of the $2J + 1$ degeneracy of the free ion states (see Figure 1.2).

This is an immediate consequence of the lowering of the symmetry as, even in the regular octahedral geometry, group theory tells us that the highest dimension of the irreducible representation is three. This is the basis of Crystal Field Theory, whose deeply symmetry-based formalism was developed by Bethe in 1929 [16].

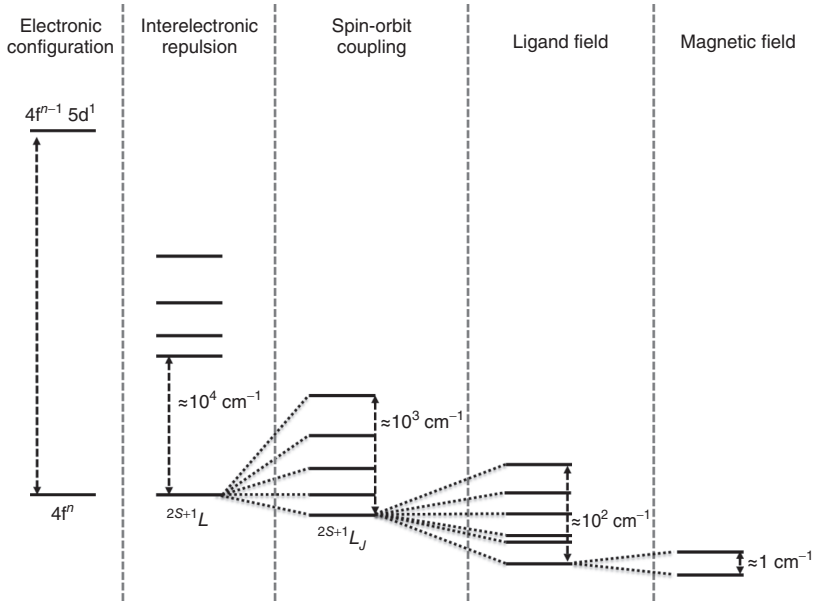

Figure 1.2 Energetic structure of a Kramers lanthanide ion in a ligand field evidencing the effect of progressively weaker perturbation. The magnetic field effect is estimated assuming a 1 T field.

Within this framework, the effect of the ligand can be described by an operator U_{CF}, which is the sum of one-electron operators for all the $4f^n$ electrons of the lanthanide, which accounts for the potential created by a charge distribution $\rho(\boldsymbol{R})$ at a distance r_i:

$$\boldsymbol{U}_{CF} = -e\sum_{j=1}^{nel.} \boldsymbol{U}_j = -e\sum_{j=1}^{nel.} \int \frac{\rho(\boldsymbol{R})}{|\boldsymbol{R} - r_i|} dv \tag{1.13}$$

The problem of evaluating the effect of the perturbation created by the ligands thus reduces to the solution of the secular determinant with matrix elements of the type $\langle\varphi_l|\boldsymbol{U}_{CF}|\varphi_k\rangle$, where $|\varphi_l\rangle$ and $|\varphi_k\rangle$ identify the eigenfunctions of the free ion. Since $|\varphi_l\rangle$ and $|\varphi_k\rangle$ are spherically symmetric, and can be expressed in terms of spherical harmonics, the potential is expanded in terms of spherical harmonics to fully exploit the symmetry of the system in evaluating these matrix elements. In detail, two different formalisms have been developed in the past to deal with the calculation of matrix elements of Equation 1.13 [2, 3]. Since U_{CF} is the sum of one-electron operators, while $|\varphi_l\rangle$ and $|\varphi_k\rangle$ are many-electron functions, both the formalisms require decomposition of free ion terms in linear combinations of monoelectronic functions.

1.3.1
Stevens' Formalism

Stevens' [2] first noted that the electrostatic potential fulfilling the symmetry requirements of the lanthanide site can be conveniently expressed as the product of a radial function and of Legendre polynomials, and thus transforms according to an irreducible representation of the rotation group. It is then possible to find a suitable constant to express such matrix elements by using an operator equivalent approach, in which the potential is expanded in a sum of equivalent angular momentum operators. In this approach, the matrix elements can be easily computed if mixing between different J multiplets is neglected. The resulting expression for Equation 1.13 using the Stevens' formalism is

$$\boldsymbol{U}_{\mathrm{CF}} = \widehat{\boldsymbol{H}}_{\mathrm{CF}}^{\mathrm{Stev}} = \sum_{k=2,4,6} \rho^k \sum_{q=-k}^{k} A_k^q \langle r^k \rangle \widehat{\boldsymbol{O}}_k^q \tag{1.14}$$

In Equation 1.14, $A_k^q\langle r^k\rangle$ is a parameter, $\widehat{\boldsymbol{O}}_k^q$ is the operator equivalent of the crystal field potential and ρ^k *is* a number which is different for the different f^n configurations and for the different k values. This accounts for the proportionality between the electrostatic potential, expressed as a spherical harmonic of order k, and the corresponding operator equivalent for that configuration [2, 6]. We note here that the number of q terms with $q \neq 0$ to be included is limited by the point group of the rare-earth site, since the CF Hamiltonian has to be invariant under all symmetry operations of the point group. The non-vanishing CF parameters in sites with commonly occurring point symmetries are reported in Table 1.2 [17, 18].

It is worth noting here that negative q values correspond to complex operators, while Stevens' parameters are always real [19]. The forms of the operator equivalents are reported in Table 1.3 [20], and the corresponding matrix elements are found tabulated in books by Abragam and Bleaney and by Altshuler [6, 21].

1.3.2
Wybourne's Formalism

Stevens' formalism turned out to be very powerful, and works easily as long as only the ground $^{2S+1}L_J$ multiplet of the lanthanide ion is considered. As such, it has been widely used in studies on EPR properties of lanthanide-based inorganic systems [6, 22], while it is not well suited for optical spectroscopy. Indeed, when starting to include excited multiplets the Stevens' formalism becomes much too involved. This is the reason why a more general formalism, developed by Wybourne [3], is of widespread use in optical studies – naturally dealing with excited multiplets – and

Table 1.2 Non-vanishing crystal field terms (Stevens' formalism) for common lanthanide point symmetries.

k	$\|q\|$	D_{3h} D_{6h} C_{6v}	C_6 C_{3h} C_{6h}	D_{2d} D_{4h} C_{4v}	S_4 C_{4h}	D_{3d} C_{3v}	C_3 S_6	D_{2h} C_{2v}	C_{2h} C_s
2	2							+	±
4	2							+	±
4	3					+	±		
4	4			+	±			+	±
6	2							+	±
6	3					+	±		
6	4			+	±			+	±
6	6	+	±			+	±	+	±

When only $q > 0$ are non-vanishing, the entry is indicated by '+', while ± indicates that both $q > 0$ and $q < 0$ terms are non-zero.

Table 1.3 Stevens' operators expressed in terms of J_+, J_-, J_z polynomials.

k	q	$\hat{O}_k^q$
2	0	$3\hat{J}_z^2 - J(J+1)$
2	±1	$\frac{\{\hat{J}_z, (\hat{J}_+ \pm \hat{J}_-)\}_+}{2c_\pm}$
2	±2	$\frac{\hat{J}_+^2 \pm \hat{J}_-^2}{c_\pm}$
4	0	$35\hat{J}_z^4 - [30J(J+1) - 25]\hat{J}_z^2 + 3J^2(J+1)^2 - 6J(J+1)$
4	±1	$\frac{\{[7\hat{J}_z^3 - 3J(J+1)\hat{J}_z - \hat{J}_z], (\hat{J}_+ \pm \hat{J}_-)\}_+}{2c_\pm}$
4	±2	$\frac{\{[7\hat{J}_z^2 - J(J+1) - 5)], (\hat{J}_+ \pm \hat{J}_-)\}_+}{2c_\pm}$
4	±3	$\frac{\{\hat{J}_z, (\hat{J}_+ \pm \hat{J}_-)^3\}_+}{2c_\pm}$
4	±4	$\frac{\hat{J}_+^4 \pm \hat{J}_-^4}{c_\pm}$
6	0	$231\hat{J}_z^6 - [315J(J+1) - 735]\hat{J}_z^4 + [105J^2(J+1)^2 - 525J(J+1) + 294]\hat{J}_z^2 - 5J^3(J+1)^3 + 40J^2(J+1)^2 - 60J(J+1)$
6	±1	$\frac{\{33\hat{J}_z^5 - [30J(J+1) - 15]\hat{J}_z^3 + [5J^2(J+1)^2 - 10J(J+1) + 12]\hat{J}_z, (\hat{J}_+ \pm \hat{J}_-)\}_+}{2c_\pm}$
6	±2	$\frac{\{33\hat{J}_z^4 - [18J(J+1) + 123]\hat{J}_z^2 + J^2(J+1)^2 + 10J(J+1) + 102, (\hat{J}_+^2 \pm \hat{J}_-^2)\}_+}{2c_\pm}$
6	±3	$\frac{\{11\hat{J}_z^2 - J(J+1) + 38, (\hat{J}_+^4 \pm \hat{J}_-^4)\}_+}{2c_\pm}$
6	±4	$\frac{\{11\hat{J}_z^2 - J(J+1) - 38, (\hat{J}_+^4 \pm \hat{J}_-^4)\}_+}{2c_\pm}$
6	±5	$\frac{\{\hat{J}_z, (\hat{J}_+ \pm \hat{J}_-)^5\}_+}{2c_\pm}$
6	±6	$\frac{\hat{J}_+^6 \pm \hat{J}_-^6}{c_\pm}$

$\{A, B\}_+$ is a shorthand notation for the product (AB + BA), $c_+ = 2$, $c_- = 2i$.

is becoming increasingly applied also to molecular magnetism studies [23–25]. We thus find it appropriate to discuss it in this section.

In this approach, the ligand field potential is expressed as

$$\begin{aligned}\boldsymbol{U}_{\mathrm{CF}} &= \widehat{\boldsymbol{H}}_{\mathrm{CF}}^{\mathrm{Wyb}} \\ &= \sum_{k=0}^{\infty}\left[B_0^0 C_0^0\,(i)+\sum_{q=1}^{k} B_q^k (C_{-q}^k(i)+(-1)^q C_q^k(i))+iB'^k_q (C_{-q}^k(i)-(-1)^q C_q^k(i))\right]\end{aligned} \tag{1.15}$$

In Equation 1.15, B_q^k and B'^k_q are the crystal field coefficients, which are all real, and $C_q^k(i)$ are tensor operators, related to the spherical harmonics $Y_q^k(i)$ by

$$C_q^k(i) = \sqrt{\frac{4\pi}{2k+1}}\, Y_q^k(i) \tag{1.16}$$

In much the same way as Stevens' operators, the summation in Equation 1.15 is limited to well-defined values: for f-electrons, the restriction $k \leq 7$ holds, while q is limited to those values consistent with the point symmetry of the site. Finally, the even part ($k = 0, 2, 4, 6$) is responsible for the CF splitting, while the odd part ($k = 1, 3, 5, 7$) is responsible for the intensity of induced electric dipole transitions in optical spectroscopy [5b, 26].

Crystal field energy levels can be found by diagonalizing the corresponding matrix, which is made up by elements of the type:

$$\langle l^n \tau S L J M_J | \widehat{\boldsymbol{H}}_{\mathrm{CF}}^{\mathrm{Wyb}} | l^{n\prime} \tau' S' L' J' M'_J \rangle \tag{1.17}$$

For low enough symmetries, both B_q^k and B'^k_q coefficients will be present in Equation 1.15, so that Equation 1.17 will be, in those cases, complex quantities. We finally note that the coefficients are transformed into CF parameters by multiplying them by the radial parts of the wave functions, represented by $R_{nl}(r)$, on which the tensor operators do not act.

Calculation of the angular part of the matrix elements thus remains, which can be performed exactly using tensor algebra techniques based on group theory. Since the calculation of the matrix elements is not straightforward, we provide here some details on it for the interested reader. The treatment follows the procedure described in Ref. [17].

The matrix element

$$\langle l^n \tau S L J M_J | \sum_i C_q^k(i) | l^{n\prime} \tau' S' L' J' M'_J \rangle \tag{1.18}$$

can be rewritten in terms of a unit tensor U_q^k as

$$\langle l^n \tau S L J M_J | U_q^k | l^{n\prime} \tau' S' L' J' M'_J \rangle \langle l \| C^k \| l' \rangle \tag{1.19}$$

The second term of the product is a reduced matrix element which contains the l-state dependence of the f electrons: since only $4f^n$ configuration, for which $l = 3$,

is considered, it can be rewritten making use of Wigner–Eckart theorem and 3-*j* symbols for the coupling of angular momenta as

$$\langle l\|C^k\|l\rangle = (-1)^l[(2l+1)(2l'+1)]^{\frac{1}{2}}\begin{pmatrix} l & k & l' \\ 0 & 0 & 0 \end{pmatrix} = -7\begin{pmatrix} 3 & k & 0 \\ 0 & 0 & 0 \end{pmatrix} \quad (1.20)$$

Using a similar approach, the first member of the product (Equation 1.19) may be rewritten as

$$\langle l^n\tau SLJM_J|U_k^q|l^{n\prime}\tau' SL'J'M_J'\rangle = (-1)^{J-M_J}\begin{pmatrix} J & k & J' \\ -M_J & q & M_J' \end{pmatrix}\langle l^n\tau SLJ\|U^k\|l^{n\prime}\tau' SL'J'\rangle \quad (1.21)$$

where the last term is a reduced matrix element, and is independent of M_J, q and M_J. Equation 1.21 can be further simplified by making use of Wigner 6-*j* symbols and a doubly reduced matrix element, obtaining:

$$\langle l^n\tau SLJM_J|U_k^q|l^{n\prime}\tau' SL'J'M_J'\rangle = (-1)^{S+L'+J+k}[(2J+1)(2J'+1)]^{\frac{1}{2}} \begin{Bmatrix} J & J' & k \\ L & L & S \end{Bmatrix}\langle l^n\tau SL\|U^k\|l^{n\prime}\tau' SL'\rangle \quad (1.22)$$

The last term on the right in Equation 1.22 represents a doubly reduced matrix element, which can be calculated by recursive formula in terms of the *coefficients of fractional parentage* [4, 14], tabulated in the work of Nielson and Koster [27]. Finally, Equation 1.18 is rewritten as

$$\begin{aligned}\langle l^n\tau SLJM_J|\sum_i C_q^k(i)|l^{n\prime}\tau' S'L'J'M_J'\rangle &= (-1)^{S+L'+2J-M_J+k+1}7[(2J+1)(2J'+1)]^{\frac{1}{2}}\begin{pmatrix} 3 & k & 3 \\ 0 & 0 & 0 \end{pmatrix} \\ &\times\begin{pmatrix} J & k & J' \\ -M_J & q & M_J' \end{pmatrix}\begin{Bmatrix} J & J' & k \\ L & L & S \end{Bmatrix}\langle l^n\tau SL\|U^k\|l^{n\prime}\tau' SL'\rangle \end{aligned} \quad (1.23)$$

Inspection of Equation 1.23 and consideration of the properties of 3-*j* and 6-*j* symbols confirm that only even k-values contribute to crystal field splitting. Further, it indicates that mixing between levels belonging to different J multiplets can only occur if terms with $k \leq J + J'$ and $-M_J + q + M_J' = 0$ are allowed by the site symmetry of the lanthanide, in much the same way as discussed above for the Stevens' formalism.

The advantage in using the Wybourne's approach in molecular magnetism is that it may provide a direct comparison with data obtained by optical spectroscopy, which is the most accurate technique for determination of the electronic structure of lanthanide ions. The application of this technique to molecular systems is just beginning, and while usually only the ground J multiplet is considered in the interpretation of the magnetic properties, the coupling of excited states can provide important effects on the wavefunction composition, thus affecting both static and dynamic magnetic properties of lanthanide-containing systems. In this

respect, complementing the results of magnetic and EPR spectroscopy with those obtained by luminescence spectroscopy can provide detailed information on the energy pattern of 4f-containing systems. This approach is still seldom applied to the study of molecular magnets, but it has been shown in past few years to provide a much improved understanding of the relation between the electronic structure and the peculiar magnetic behaviour of these systems [28–30].

1.3.3
Standardization

When treating CF parameters in any of the two formalisms, non-specialists often overlook that the coefficients of the expansion of the CF potential (i.e. the values of CF parameters) depend on the choice of the coordinate system, so that conventions for assigning the correct reference framework are required. The conventional choice in which parameters are expressed requires the z-direction to be the principal symmetry axis, while the y-axis is chosen to coincide with a twofold symmetry axis (if present). Finally, the x-axis is perpendicular to both y- and z-axes, in such a way that the three axes form a right-handed coordinate system [31]. For symmetry in which no binary axis perpendicular to principal symmetry axis exists (e.g. C_{3h}, C_{4h}), y is usually chosen so as to set one of the B'^{k}_{q} (in Wybourne's approach) or A^{q}_{k} with $q < 0$ (in Stevens' approach) to zero, thereby reducing the number of terms providing a non-zero imaginary contribution to the matrix elements of the ligand field Hamiltonian. Finally, for even lower symmetry (orthorhombic or monoclinic), the correct choice is such that the ratio of the Stevens' parameter is restrained to $\lambda' = A^0_2/A^2_2 \in (0, \pm 1)$ and equivalently $\kappa = B^0_2/B^2_2 \in (0, \pm 1/\sqrt{6})$ in the Wybourne's notation [19, 32]. If literature-reported or experimentally determined parameters do not conform to this convention, rotation of the reference system should be applied, resulting in a standardized form of CF parameters [33]. This is of fundamental importance if different sets of parameters are to be compared to derive magnetostructural correlations and the direction of the quantization axis, and thus of the principal anisotropy axis, appropriately defined.

1.3.4
Calculation of Crystal Field Parameters

It is evident that the approach described so far to derive the electronic structure of lanthanide ions, based on perturbation theory, requires a large number of parameters to be determined. While state-of-the-art *ab initio* calculation procedures, based on complete active space self consistent field (CASSCF) approach, are reaching an extremely high degree of accuracy [34–37], the CF approach remains widely used, especially in spectroscopic studies. However, for low point symmetry, such as those commonly observed in molecular complexes, the number of CF

parameters to be determined is as high as 27 (for C_i symmetry), which is clearly too large to be meaningful. To reduce the number of free parameters in the fit of either spectroscopic or magnetic data, some kind of *ab initio* calculation on the CF parameters is clearly necessary and we present here the basic concepts underlying some of them. Such calculations usually require the use of structural parameters (e.g. length and orientation of lanthanide–ligand atom distance with respect to a defined reference frame), and the determination of parameters describing the charge distribution on the ligand (or the ligand–lanthanide interaction in a molecular orbital oriented description), which should be consistent with chemical intuition.

The simplest approximation is that of considering a point-charge electrostatic model (PCEM), which parameterizes the crystal field effect generated by the n atoms coordinated to the lanthanide by using n point charges placed at the corresponding atomic positions. In other words, one may express Equation 1.13 as

$$\boldsymbol{u}_{\mathrm{CF}} = \sum_{j=1}^{nel.} \sum_{i=1}^{nlig} \frac{Z_i e^2}{r_{ij}} \tag{1.24}$$

The corresponding parameters obtained by this assumption do not provide, with some exceptions [38], acceptable fits to the experimentally available data for lanthanide-based molecular magnets. Indeed, such a model neglects the degree of covalent interaction of the metal–ligand configuration, and is thus only justified for ionic compounds. The situation for lanthanide(III) ions in a molecular compound with organic ligands can be rather different, and it has been already evidenced that for such compounds the CF can be strongly affected by covalency. Among the applications of models which take into account covalence to molecular magnets, it is worth mentioning the determination of CF parameters by using the simple overlap model. In this model, the ligand field is calculated by considering effective charges, located in the middle of the Ln–ligand bond, which are proportional to the total overlap between lanthanide and ligand wave functions and to charge factors [39]. Among other systems, this model has been successfully applied to rationalize the magnetic properties of holmium–nitrone complexes, which were then used as a starting point for the analysis of the exchange coupling in Ho-nitronyl nitroxide systems [40].

More recently, Coronado *et al.* [41] suggested a radial effective charge (REC) model, in which the effect of the ligating atom is modelled through an effective point charge situated along the lanthanide–ligand axis at a distance R, which is a parametric distance smaller than the real metal–ligand distance. At the same time, the charge value (q) is scanned in order to achieve the minimum deviation between calculated and experimental data. This was shown to work quite well for halide ligands, due to the spherical character of the electron density in the coordinating atom, while a lone pair covalent effective charge (LPEC) model

was needed in the case of nitrogen ligands. In the latter case, a further displacement parameter was needed in order to account for the mismatch between the orientation of the nitrogen lone pair and the Ln–N direction. This model was used to explain the results obtained in one of the most common classes of single-ion magnet (SIM), namely lanthanide phthalocyanine sandwich complexes [41b]. Promising results on these systems have been obtained also by Klokishner *et al*. [42] by using the exchange-charge model [43], which considers both the interaction of the 4f electrons with the point charges of the surrounding ligands, and the overlap of the 4f orbitals with the ligand orbitals to contribute to the ligand field.

Among the most relevant approaches in the description of electronic properties of lanthanides is surely the angular overlap model (AOM) [44, 45]. The key idea underlying the model is best explained by looking at the main assumptions characterizing the AOM: (i) The energy of any f orbital E_f is obtained as a perturbation, which is proportional to the squares of metal–ligand overlap integrals. (ii) If the basis of the f-orbitals is defined relative to a coordinate system *xyz*, then the perturbation matrix due to a ligand placed on *z* is diagonal. (iii) Contributions arising from different ligands are additive.

The parameters describing the interaction between the ligand and the lanthanide are directly related to the σ-, π-, δ- and φ-bonding ability of the ligands, which may be influenced by the synthetic chemist. Moreover it is, in principle, possible to calculate the effect of the ligand by using the real coordination geometry around the metal ion site, thus including effects due to the low symmetry of the ligand field. The relations between angular overlap parameters and CF parameters was first reported by Urland for the case of isotropic π-ligands [44b]. This was successfully improved by including anisotropic π-ligands and applied to the interpretation of susceptibility, electronic and EPR spectra of $[Ph_4As]_2[Yb(NO_3)_5]$ [46] and of the extremely well-characterized series of $[Ln(H_2O)_9][EtOSO_3]$, which showed that electrostatic effects due to neighbouring complexes become relevant in the determination of axial second-order ligand field parameters [47]. More recently, Flanagan *et al*. [45] provided relations which also include anisotropic π-ligands, and applied the AOM to a global fit of CF parameters derived by polarized luminescence spectroscopy. This approach was used for the series of homologous compounds Ln(trensal) (where H_3trensal = 2, 2′, 2″-tris(salicylideneimino)triethylamine), where the variations of the AOM parameters were related to the small structural changes observed along the series. In particular, it was concluded that the metal–ligand overlap decreases on moving across the series as the result of the contraction of the f orbitals, which overcomes the effect of the decreasing bond lengths.

Finally, we note that even if in these studies only e_σ and e_π parameters were used for the description of the ligand field, we have recently shown, by applying AOM to the interpretation of the magnetic properties of Dy^{3+} derivatives of both

polyoxometallate and phthalocyaninate, that e_δ cannot always be considered as negligible [48].

1.4 Magnetic Properties of Isolated Lanthanide Ions

1.4.1 Effect of a Magnetic Field

The application of a magnetic field to the wavefunctions obtained by the procedure described in the previous sections results in the complete removal of the degeneracy of the J multiplet, either pertaining to Kramers or non-Kramers ions, and yields a temperature-dependent population of the different $2J + 1$ components (Figure 1.2) Thus, at low temperatures, large deviations from the Curie law are observed. The effect of the magnetic field is described by the Zeeman Hamiltonian:

$$\hat{H}_{\text{Zeem}} = -\hat{\boldsymbol{\mu}} \cdot \boldsymbol{B} \tag{1.25}$$

where

$$\hat{\boldsymbol{\mu}} = -\mu_{\text{B}}[(\hat{L}_x + 2\hat{S}_x)\boldsymbol{i} + (\hat{L}_y + 2\hat{S}_y)\boldsymbol{j} + (\hat{L}_z + 2\hat{S}_z)\boldsymbol{k}] \tag{1.26}$$

For a general orientation α of the magnetic field B, with intensity $|B|$ and components (B_x, B_y, B_z), Equation 1.25 can be rewritten as

$$\hat{H}_{\text{Zeem},\alpha} = \mu_{\text{B}}[(\hat{L}_x + 2\hat{S}_x)B_x + (\hat{L}_y + 2\hat{S}_y)B_y + (\hat{L}_z + 2\hat{S}_z)B_z] \tag{1.27}$$

The effect of $\hat{H}_{\text{Zeem},\alpha}$ is evaluated by applying it to the eigenfunctions resulting from the crystal field analysis, which provides the eigenvectors $|n_\alpha\rangle$ and the energies $E_{n,\alpha}$. The resulting magnetization in a magnetic field applied along the direction α is written as

$$M_\alpha = N_{\text{A}} \frac{\sum_{n,\alpha} -\frac{\partial E_{n,\alpha}}{\partial B} \exp\left(-\frac{E_{n,\alpha}}{k_{\text{B}}T}\right)}{\sum_{n,\alpha} \exp\left(-\frac{E_{n,\alpha}}{k_{\text{B}}T}\right)} \tag{1.28}$$

where the values of $\partial E_{n,\alpha}/\partial B$ can be calculated by applying the operator $\hat{H}_{\text{Zeem},\alpha}/B$ on the eigenvectors $|n_\alpha\rangle$. As a consequence of the crystal field effects, $\partial E_{n,\alpha}/\partial B$ can be strongly dependent on α, thus providing a magnetization which can be largely anisotropic even at room temperature [49]. Single crystal measurements, of magnetization, susceptibility or torque, are then very powerful to obtain an accurate determination of CF parameters. On the other hand,

magnetic properties of powder samples are much less sensitive to CF parameters, especially the transverse ones (i.e. $q \neq 0$), so that reliable estimates can only be obtained in these cases when additional information is available (i.e. homologous series of lanthanides, further spectroscopic information). Quite often, susceptibility measurements are indeed interpreted by assuming an idealized site symmetry neglecting most of the supposedly small transverse term of the crystal field [24, 50]. This has to be accurately considered when trying to correlate the low temperature dynamic behaviour of the magnetization with the eigenvalues and eigenvectors pattern arising by static magnetic measurements.

1.4.2
EPR Spectroscopy of Lanthanide Complexes

EPR spectroscopy has been heavily applied in the past to the analysis of the magnetic properties of compounds containing ions of the rare-earth group [6]. Results obtained by this technique were indeed one of the driving forces in the derivation of a consistent theory of the crystal field. In particular, some degree of admixture of low-lying excited states in the ground state had often to be taken into account to fit the experimental data, still within a model of ionic character. Due to the unquenched orbital contribution, EPR spectra of lanthanide ions are usually observed only at low temperatures, since the resulting fast spin–lattice relaxation times hamper signal detection at higher temperatures. As a consequence, they are normally interpreted by considering that only the lowest levels arising from the ligand field splitting of the ground J multiplet are EPR active.[2)]

If the Ln^{3+} centre is a Kramers ion, the spectra can be interpreted in terms of a doublet with largely anisotropic effective g-values. If one neglects the admixture of higher lying J multiplets and considers an axial symmetry, the effective g values will be

$$g_{//} = 2g_J\langle\Psi_+|\hat{J}_z|\Psi_+\rangle$$
$$g_\perp = g_J\langle\Psi_+|\hat{J}_+|\Psi_-\rangle \tag{1.29}$$

The wavefunctions $\Psi_\pm$ can be written as

$$\Psi_\pm = \sum c_{M_J}|M_J, J\rangle \tag{1.30}$$

The number of terms retained in Equation 1.30 obviously depends on the symmetry of the ligand field: if an axis of q-fold symmetry is present, only M_J values differing by $\pm q$ will contribute to Equation 1.30. Note that for rhombic and lower symmetries, two different effective values of g are expected for the x and y directions. In this respect, EPR is extremely sensitive to transverse terms of the CF,

2) To further reduce the linewidth of the spectra, doping in isostructural Y^{3+}, La^{3+} or Lu^{3+} host is usually performed to minimize dipolar broadening and spin–spin relaxation.

since they not only alter c_{M_J} coefficients, and thus the effective g values, but may provide the only mechanism to obtain a non-zero transition probability within the doublet.

In more general terms, considering also the mixing of higher lying J states, the ground doublet wavefunction will be of the type

$$\Psi_{\pm} = \sum c_{M_J} |M_J, J\rangle + \sum c'_{M_J} |M_J, J'\rangle \tag{1.31}$$

While this generally has only small effects on the static magnetic properties, it may play a relevant role in providing a quantitative agreement with experimental resonance data, and in explaining quantum tunnelling relaxation of the magnetization at low temperature [51].

For non-Kramers lanthanide ions, the ligand field splitting may provide, depending on the symmetry, either singlets, doublets or pseudo-doublets. In this situation, spectra are usually analysed, depending on the symmetry, either as pseudo-doublets or pseudo-triplets (if the energy difference between singlet and doublet or pseudo-doublet groups of levels is relatively small) with very anisotropic g-value and a sizeable zero field splitting (ZFS) term of the effective spin Hamiltonian:

$$\widehat{H}_{\mathrm{nK}} = \mu_{\mathbf{B}} \boldsymbol{B} \cdot \boldsymbol{g} \cdot \boldsymbol{S}_{\mathbf{eff}} + \boldsymbol{S}_{\mathbf{eff}} \cdot \boldsymbol{D} \cdot \boldsymbol{S}_{\mathbf{eff}} \tag{1.32}$$

Despite the historical relevance of EPR spectroscopy in the elucidation of the electronic structure of lanthanide compounds, relatively few results have been reported in the domain of molecular magnetism. The vast majority of these studies, as will be seen hereafter, were focused on complexes of the second half of the lanthanide series, to gain more information about the slow relaxation of the magnetization in these systems. Among the few exceptions, our group reported a few powder EPR spectra of the family Ln(trp)$(HBPz_3)_2$ (where trp, tropolonate, $HBPz_3$, hydrotrispyrazolylborate), of which only Yb(trp)$(HBPz_3)_2$ could be fully interpreted and simulated. Despite the rhombic structural symmetry, this system provided a near-axial spectrum, indicating that the best description of the ligand field geometry is square antiprismatic with fourfold symmetry. The observed effective g-values were rationalized on the basis of this idealized geometry, and the ground doublet of Yb(trp)$(HBPz_3)_2$ turned out to be composed by $|J, M_J\rangle = |7/2, \pm 5/2\rangle$ for 98% [52].

A more complex situation was encountered in the analysis of single-crystal EPR spectra of the member of $[Ce(dmf)_4(H_2O)_3(\mu\text{-}CN)Co(CN)_5]$ (dmf, N,N'-dimethylformamide, Co = Co^{3+}) [53]. In this case, the investigation provided the orientation of the principal g-values of Ce^{3+} ground doublet, which, quite interestingly, did not show any peculiar relation to the axis of the bicapped trigonal prism formed by the ligands (Figure 1.3). Furthermore, on an analysis based on orthorhombic symmetry and the lowest $J = 5/2$ value only, Equation 1.30 yielded calculated g-values which agree with the observed values only within 12%. The observed discrepancy was attributed both to a small amount of mixing

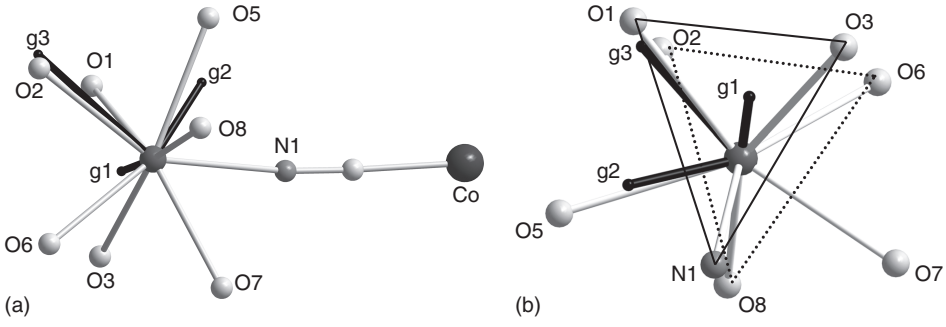

Figure 1.3 Orientation of the g tensor of Ce^{3+} in $[Ce(dmf)_4(H_2O)_3(\mu\text{-}CN)Co(CN)_5]$ with respect to the bicapped trigonal prism of the coordination sphere of Ce^{3+} centre (a), and with respect to the Co–C–N–Ce plane (b). For both figures, each component of the tensor is proportional to its respective modulus. (After Ref. [53], WIley-VCH.)

of the $^2F_{7/2}$ state in the ground doublet and to the simplifying assumption of orthorhombic symmetry.

The importance of EPR spectroscopy in evidencing low-symmetry terms of the CF was reported by one of us, in collaboration with the group of Boskovic and Kogerler [24], in the investigation of a Dy^{3+} polyoxometallate, based on the $[As_2W_{19}O_{67}(H_2O)]^{14-}$ anion. X-band EPR spectra were strongly temperature dependent, with a signal reaching a maximum intensity around 40 K: on the basis of the fit of magnetic susceptibility, which neglected the transverse CF terms, this was assigned to a doublet with prevailing $M_J = \pm 9/2$ component, which, according to ligand field calculations, lies 34 K above the ground state. The observation of an EPR spectrum with $g_\perp \neq 0$ demonstrated unequivocally that the transverse fourth-order ligand-field components are non-zero, since these terms provide the only means to observe a non-zero perpendicular component of the spectrum. Calculation based on Equations 1.29 – 1.30 suggested that a rather large mixing is induced by these terms, indicating the importance of spectroscopic information complementing the thermodynamic ones in providing an accurate picture of the electronic structure of these systems. A similar phenomenon was more recently observed by Schelter and coworkers [54], who performed X-band EPR spectroscopy on two of the Dy^{3+} complexes, showing that, while the ground state was essentially $M_J = \pm 13/2$ in nature, non-negligible mixing due to low symmetry components of the ligand field occurred.

Finally, we note that, to the best of our knowledge, only one report exists about EPR spectra of non-Kramers lanthanide ions in molecular magnets. In 2012, Hill and coworkers [51] performed a multifrequency study on powder and single crystal samples of $Na_9Ho(W_5O_{18})_2 \cdot nH_2O$, in both the pure form and when doped into the isostructural Y^{3+} derivative. While crystallizing in a triclinic unit cell, the symmetry of the lanthanide ion in this family is very close to D_{4d}. For this reason, susceptibility data had been previously fitted by a purely axial Hamiltonian [50].

However, consistent explanation of the EPR properties of the Ho^{3+} derivative required the inclusion of at least transverse fourth-order terms. The parameters obtained by accurate single-crystal EPR simulations confirmed the dominant $M_J = \pm 4$ character of the ground pseudo-doublet, which is separated by about $16\,cm^{-1}$ from the first excited state, of essentially $M_J = \pm 5$ character. More important, however, is that the two components of the ground state are partially split both by a fourth-order transverse term and by hyperfine interaction with the $I = 7/2$ Ho nucleus, resulting in the pattern outlined in Figure 1.4. In particular, the former terms are the only ones capable of explaining the actual observation of non-zero intensity in the EPR spectrum. Furthermore, they are very efficient (to just the second-order of perturbation) in mixing the two components of the ground state, thus explaining the field-dependent spin dynamics of this system. Such studies clearly highlight the relevance of EPR techniques in unveiling subtle details of the electronic structure of lanthanide-based molecular magnets, which are otherwise inaccessible by magnetic characterization. This is of paramount importance in determining the key factors affecting their low temperature spin dynamics. In particular, the possibility of having access to details of hyperfine interaction may be of much relevance to the explanation of hyperfine mediated tunnelling relaxation [55, 56].

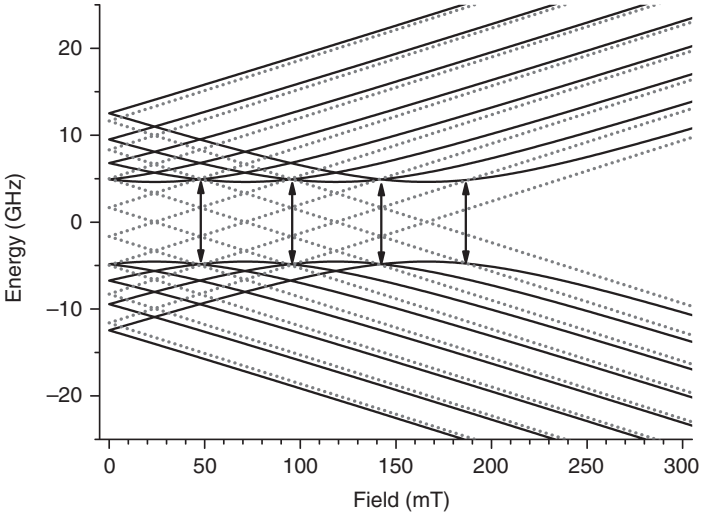

Figure 1.4 Plot of the lowest hyperfine split pseudo-doublet for field applied along the easy magnetization axis of $Na_9Ho(W_5O_{18})_2 \cdot nH_2O$. Grey dotted lines are obtained in the assumption of purely axial symmetry while black continuous lines result after inclusion of symmetry allowed fourth-order transverse anisotropy. Black arrows represent the calculated resonance position in the latter assumption for X-band frequency. (Redrawn using original data reported in Ref. [51], Royal Society of Chemistry.)

1.5
Exchange Coupling in Systems Containing Orbitally Degenerate Lanthanides

Up to now, we have only treated systems containing a single lanthanide ion. We wish to introduce here some of the problems which are encountered when dealing with exchange coupling in systems containing orbitally degenerate ions. The main problem in evaluating the exchange coupling in such compounds lies in the fact that one cannot use the isotropic spin Hamiltonian approach which is normally adopted to parameterize the magnetic interactions in compounds containing orbitally non-degenerate centres [57]. Indeed, when systems with unquenched angular orbital momentum are considered, S is no longer a good quantum number, and the energies of the levels depend also on the value of M_S, with $-S \leq M_S \leq S$, that is, there will be some preferential orientation of the magnetic moment even in zero field. This is the main reason for the peculiar difficulties arising in the analysis of the magnetic behaviour of the lanthanides. The first detailed and quantitative treatment of the interactions involving one orbitally non-degenerate ion, such as Fe^{3+}, and an orbitally degenerate lanthanide ion was performed by Levy [58] in an attempt to rationalize the exchange interactions in Yb^{3+} garnets, and was later employed by Yamaguchi and Kamimura [59] to analyse the behaviour of Ho^{3+} garnets. The assumptions on which this approach relies are (i) that the spin dependence of the superexchange interaction between a 4f electron and the orbitally non-degenerate state ions is well described by the Dirac–Van Vleck Hamiltonian and (ii) that the dependence of this interaction on the orbital state of the lanthanide is accounted for by an exchange potential. The exchange interaction is then described by an anisotropic exchange Hamiltonian exploiting the formalism of irreducible tensor operators $T_q^{[k]}$:

$$\hat{\boldsymbol{H}}_{\text{exc}} = \sum_{k=0}^{2l} \sum_{q=-k}^{k} \alpha_{kq} \boldsymbol{T}_q^{[k]}(i) \boldsymbol{s}(i) \cdot \boldsymbol{S}(TM) \tag{1.33}$$

where $l = 3$ for lanthanides, i indicates the i-th electron of the lanthanide ion, $S(TM)$ is the spin operator of the transition metal ion and α_{kq} are the exchange coupling parameters, α_{00} being the isotropic one. Furthermore, it is necessary to know the wavefunctions of the lanthanide (and thus the relative coefficient of S values entering Equation 1.33 in the absence of exchange, which can be obtained by the CF parameters as discussed in Section 1.3). It is evident that the number of adjustable parameters is now huge, especially in the low site symmetry usually characteristic of molecular complexes of Ln^{3+}, and a meaningful fit of the experimental parameters becomes extremely difficult. Furthermore, it is in principle absolutely necessary to perform orientation-dependent measurements because the global Hamiltonian, including both exchange and single ion contributions, is intrinsically anisotropic. For this reason, there have been no reports of the application of this approach to molecular complexes, after

the series of papers by the Florence University group [60], which synthesized and magnetically characterized different copper–lanthanide molecular complexes. CF parameters were obtained by an independent fit of the powder magnetic susceptibility of $[Ln(hfac)_3(H_2O)_2]$ (hfac, hexafluoroacetylacetonate) and fixed in order to reduce the parameterization of the system. It was then possible to find out that the isotropic term of the coupling Hamiltonian was antiferromagnetic while the anisotropic ones were ferromagnetic: to reduce the number of parameters, however, only second-order anisotropic exchange was considered.

More often, a simple qualitative approach has been used to get information on the nature of the interaction (ferro- or antiferromagnetic) in lanthanides coupled to organic radicals or to copper(II). Within this approach, the exchange interaction in coupled systems is made apparent by subtracting from χT of the complex the contribution arising from the thermal depopulation of the M_j sublevels of Ln^{3+}, $\chi_{Ln}T$, which is obtained by measuring an isostructural Ln^{3+} complex with a diamagnetic surrounding. This approach has been successfully applied both to the investigation of 4f–3d couples, for example, by replacing the paramagnetic copper(II) by a square-planar nickel(II) or zinc(II), and to 4f–2p complexes, where the organic radical was substituted by a diamagnetic ligand analogue carrying the same charge [52, 61–63].

Extension of this approach to quantitative estimation of the exchange coupling has also been reported by different groups [40, 42] by fitting the data of the diamagnetic substitute analogue with one of the CF calculation models described in Section 1.3.4. This allows derivation of the eigenfunctions and eigenvalues of the ground multiplet of the isolated lanthanide. The exchange interaction is subsequently evaluated in the assumption of isotropic coupling, which is often sufficient to yield a reasonable fit of the powder susceptibility.

As powerful as it can be, the diamagnetic substitution approach does not provide reliable information about the anisotropic features of the exchange between the species involved if only powder measurements are considered. We have recently demonstrated this by an integrated single crystal EPR and magnetic study on the $[Ln(dmf)_4(H_2O)_3(\mu\text{-}CN)M(CN)_5]$ family discussed above, with $M = Co^{3+}$, Fe^{3+} and Ln = La, Ce. Investigation of the two members of the family containing one paramagnetic centre resulted in a detailed picture of the low-lying levels of Ce^{3+} and Fe^{3+} ions. Analysis of the coupled species performed using this piece of information clearly indicated that a sound explanation of the data required the inclusion of isotropic, anisotropic and antisymmetric terms to describe the exchange interaction among the doublets [53].

Acknowledgements

We are grateful to Prof. R. Sessoli, Prof. C. Benelli, Mrs. E. Lucaccini and Mr. M. Perfetti for stimulating discussions.

References

1. Becquerel, J. (1908) *Le Radium*, **5**, 5–17.
2. Stevens, K.W.H. (1952) *Proc. Phys. Soc. London, Sect. A*, **65**, 209–215.
3. Wybourne, B.G. (1965) *Spectroscopic Properties of Rare Earths*, John Wiley & Sons, Inc., New York.
4. Judd, B.R. (1963) *Operator Techniques in Atomic Spectroscopy*, McGraw-Hill, New York.
5. (a) Ofelt, G.S. (1963) *J. Chem. Phys.*, **38**, 2171–2180; (b) Ofelt, G.S. (1962) *J. Chem. Phys.*, **37**, 511–520.
6. Abragam, A. and Bleaney, B. (1970) *Electron Paramagnetic Resonance of Transition Ions*, Clarendon Press, Oxford.
7. Dieke, G.H. and Crosswhite, H. (1968) *Crosswhite Spectra and Energy Levels of Rare Earth Ions in Crystals*, Interscience Publishers, New York.
8. Kahn, O. (1993) *Molecular Magnetism*, Wiley-VCH Verlag GmbH, New York.
9. Van Vleck, J.H. (1932) *The Theory of Electric and Paramagnetic Susceptibilities*, Oxford University Press, Oxford.
10. Hund, F. (1925) *Z. Phys.*, **33**, 855–859.
11. Laporte, O. (1928) *Z. Phys.*, **47**, 761–769.
12. (a) Van Vleck, J.H. and Frank, A. (1929) *Phys. Rev.*, **34**, 1494–1496; (b) Van Vleck, J.H. and Frank, A. (1929) *Phys. Rev.*, **34**, 1625–1625.
13. (a) Slater, J.C. (1929) *Phys. Rev.*, **34**, 1293–1322; (b) Condon, E.U. and Shortley, G.H. (1951) *The Theory of Atomic Spectra*, Cambridge University Press, Cambridge.
14. Racah, G. (1949) *Phys. Rev.*, **76**, 1352–1365.
15. Casey, A.T. and Mitra, S. (1976) in *Theory and Applications of Molecular Paramagnetism* (eds E.A. Boudreaux and L.N. Mulay), Wiley-Interscience, New York, 271–316.
16. Bethe, H. (1929) *Ann. Phys.*, **395**, 133–208.
17. Gorller-Walrand, C. and Binnemans, K. (1996) Rationalization of crystal-field parametrization, in *Handbook On the Physics and Chemistry of Rare Earths*, vol. 23 (eds K.A. Gschneidner and L. Eyring), Elsevier, Amsterdam.
18. Newman, D.J. and Ng, B. (2000) Empirical crystal fields, in *Crystal Field Handbook* (eds D.J. Newman and B. Ng), Cambridge University Press, Cambridge.
19. Rudowicz, C. (1986) *J. Chem. Phys.*, **84**, 5045–5058.
20. Rudowicz, C. and Chung, C.Y. (2004) *J. Phys. Condens. Matter*, **16**, 1–23.
21. Altshuler, S.A. and Kozyrev, B.M. (1974) *Electron Paramagnetic Resonance in Compounds of Transition Elements*, 2nd edn, John Wiley & Sons, Inc., New York.
22. (a) Elliott, R.J. and Stevens, K.W.H. (1952) *Proc. R. Soc. London, Ser. A*, **215**, 437–453; (b) Elliott, R.J. and Stevens, K.W.H. (1953) *Proc. R. Soc. London, Ser. A*, **218**, 553–566; (c) Elliott, R.J. and Stevens, K.W.H. (1953) *Proc. R. Soc. London, Ser. A*, **219**, 387–404.
23. Schilder, H. and Lueken, H. (2004) *J. Magn. Magn. Mater.*, **281**, 17–26.
24. Ritchie, C., Speldrich, M., Gable, R.W., Sorace, L., Kogerler, P. and Boskovic, C. (2011) *Inorg. Chem.*, **50**, 7004–7014.
25. Reu, O., Palii, A., Ostrovsky, S., Wallace, W., Zaharko, O., Chandrasekhar, V., Clerac, R. and Klokishner, S. (2013) *J. Phys. Chem. C*, **117**, 6880–6888.
26. Judd, B.R. (1962) *Phys. Rev.*, **127**, 750–761.
27. Nielson, C.W. and Koster, G.F. (1963) *Spectroscopic Coefficients for the p^n*,

d^n and f^n Configurations, MIT press, Boston, MA.
28. Cucinotta, G., Perfetti, M., Luzon, J., Car, P.-E., Mael, E., Caneschi, A., Calvez, G., Bernot, K. and Sessoli, R. (2012) *Angew. Chem. Int. Ed.*, **51**, 1606–1610.
29. Rinehart, J.D. and Long, J.R. (2012) *Dalton Trans.*, **41**, 13572–13574.
30. (a) Lucaccini, E., Sorace, L., Perfetti, M., Costes, J.-P. and Sessoli, R. (2014) *Chem. Commun.*, **50**, 1648–1651; (b) Pedersen, K.S., Ungur, L., Sigrist, M., Sundt, A., Schau-Magnussen, M., Vieru, V., Mutka, H., Rols, S., Weihe, H., Waldmann, O., Chibotaru, L.F., Bendix, J. and Dreiser, J. (2014) *Chem. Sci.*, **5**, 1650.
31. Prather, J.L. (1961) *Atomic Energy Levels in Crystals*, National Bureau of Standards Monograph, U.S. National Bureau of Standards, Washington, DC.
32. Rudowicz, C., Chua, M. and Reid, M.F. (2000) *Physica B*, **291**, 327–338.
33. Rudowicz, C. (1985) *J. Phys. C: Solid State Phys.*, **18**, 1415–1430.
34. Chibotaru, L.F., Ungur, L. and Soncini, A. (2008) *Angew. Chem. Int. Ed.*, **47**, 4126–4129.
35. Luzon, J., Bernot, K., Hewitt, I., Anson, C., Sessoli, R. and Powell, A.K. (2008) *Phys. Rev. Lett.*, **100**, e247205.
36. Ungur, L. and Chibotaru, L.F. (2011) *Phys. Chem. Chem. Phys.*, **13**, 20086–20090.
37. Boulon, M.E., Cucinotta, G., Luzon, J., Degl'Innocenti, C., Perfetti, M., Bernot, K., Calvez, G., Caneschi, A. and Sessoli, R. (2013) *Angew. Chem. Int. Ed.*, **52**, 350.
38. Baldoví, J.J., Cardona-Serra, S., Clemente-Juan, J.M., Coronado, E. and Gaita-Ariño, A. (2012) *Inorg. Chem.*, **51**, 12565–12574.
39. Porcher, P., Dos Santos, M.C. and Malta, O. (1999) *Phys. Chem. Chem. Phys.*, **1**, 397.
40. Kahn, M.L., Ballou, R., Porcher, P., Kahn, O. and Sutter, J.P. (2002) *Chem. Eur. J.*, **8**, 525.
41. (a) Baldoví, J.J., Cardona-Serra, S., Clemente-Juan, J.M., Coronado, E., Gaita-Ariño, A. and Palii, A. (2013) *J. Comput. Chem.*, **34**, 1961–1967; (b) Baldovi, J.J., Clemente-Juan, J.M., Coronado, E. and Gaita-Ariño, A. (2012) *Dalton Trans.*, **41**, 13705–13713.
42. Reu, O.S., Palii, A.V., Ostrovsky, S.M., Tregenna-Piggott, P.L.W. and Klokishner, S.I. (2012) *Inorg. Chem.*, **51**, 10955–10965.
43. Popova, M.N., Chukalina, E.P., Malkin, B.Z. and Saikin, S.K. (2000) *Phys. Rev. B*, **61**, 7421.
44. (a) Jørgensen, C.K., Pappalardo, R. and Schmidtke, H.-H. (1963) *J. Chem. Phys.*, **39**, 1422; (b) Urland, W. (1976) *Chem. Phys.*, **14**, 393–401.
45. Flanagan, B.M., Bernhardt, P.V., Luthi, S.R., Riley, M.J. and Krausz, E.R. (2001) *Inorg. Chem.*, **40**, 5401.
46. Urland, W. and Kremer, R. (1984) *Inorg. Chem.*, **23**, 1550–1553.
47. Urland, W. (1979) *Chem. Phys. Lett.*, **62**, 525–528.
48. Sorace, L., Benelli, C. and Gatteschi, D. (2011) *Chem. Soc. Rev.*, **40**, 3092–3104.
49. Mironov, V.S., Galyametdinov, Y.G., Ceulemans, A., Gorller-Walrand, C. and Binnemans, K. (2002) *J. Chem. Phys.*, **116**, 4673–4685.
50. AlDamen, M.A., Clemente Juan, J.M., Coronado, E., Martì-Gastaldo, C. and Gaita-Ariño, A. (2008) *J. Am. Chem. Soc.*, **130**, 8874–8875.
51. Ghosh, S., Datta, S., Friend, L., Cardona-Serra, S., Gaita-Ariño, A., Coronado, E. and Hill, S. (2012) *Dalton Trans.*, **41**, 13697–13704.
52. Caneschi, A., Dei, A., Gatteschi, D., Poussereau, S. and Sorace, L. (2004) *Dalton Trans.*, 1048–1055.
53. Sorace, L., Sangregorio, C., Figuerola, A., Benelli, C. and Gatteschi, D. (2009) *Chem. Eur. J.*, **15**, 1377–1388.
54. Williams, U.J., Mahoney, B.D., DeGregorio, P.T., Carroll, P.J., Nakamaru-Ogiso, E., Kikkawa, J.M. and Schelter, E.J. (2012) *Chem. Commun.*, **48**, 5593–5595.
55. Giraud, R., Wernsdorfer, W., Tkachuk, A.M., Mailly, D. and Barbara, B. (2001) *Phys. Rev. Lett.*, **87**, 057203.
56. Vincent, R., Klyatskaya, S., Ruben, M., Wernsdorfer, W. and Balestro, F. (2012) *Nature*, **488**, 357–360.

57. Borras-Almenar, J.J., Clemente-Juan, J.M., Coronado, E., Palii, A.V. and Tsukerblat, B.S. (1998) *J. Phys. Chem. A*, **102**, 200–213.

58. (a) Levy, P.M. (1964) *Phys. Rev.*, **135**, A155–A165; (b) Levy, P.M. (1966) *Phys. Rev.*, **147**, 311–319.

59. Kamimura, H. and Yamaguchi, T. (1970) *Phys. Rev. B*, **1**, 2902–2911.

60. (a) Benelli, C., Caneschi, A., Gatteschi, D., Guillou, O. and Pardi, L. (1990) *J. Magn. Magn. Mater.*, **83**, 522–524; (b) Benelli, C., Caneschi, A., Gatteschi, D., Guillou, O. and Pardi, L. (1990) *Inorg. Chem.*, **29**, 1750–1755.

61. Costes, J.P., Dahan, F., Dupuis, A. and Laurent, J.P. (1998) *Chem. Eur. J.*, **4**, 161–1620.

62. Kahn, M.L., Sutter, J.P., Golhen, S., Guionneau, P., Ouahab, L., Kahn, O. and Chasseau, D. (2000) *J. Am. Chem. Soc.*, **122**, 3413–3421.

63. Figuerola, A., Diaz, C., Ribas, J., Tangoulis, V., Lloret, F., Mahia, J. and Maestro, M. (2003) *Inorg. Chem.*, **42**, 641–649.